Dinuclear nucleobase-anion-bridged complexes of Pd^{II} and Pt^{II} with 1-methylimidazol-2-yl pyridin-2-yl ketone: synthesis, crystal structure and solution behaviour †

Holger Engelking and Bernt Krebs*

Anorganisch-Chemisches Institut der Universität Münster, Wilhelm-Klemm-Strasse 8, D-48149 Münster, Germany

The reactions of [M(mipk)(H$_2$O)$_2$]$^{2+}$ (M = Pd or Pt; mipk = 1-methylimidazol-2-yl pyridin-2-yl ketone) with the nucleobases 1-methylthymine (Hmthy) and 1-methyluracil (Hmura) were studied and the products characterized by X-ray structure analyses as well as by ^{1}H NMR spectroscopy. Dinuclear complexes are formed with the pyrimidine-based model nucleobases, which act as secondary bridging ligands *via* their N^3 and O^4 donor functions. In all three compounds [Pd$_2$(mipk)$_2$(mura)$_2$][ClO$_4$]$_2$ **1**, [Pd$_2$(mipk)$_2$(mthy)$_2$][ClO$_4$]$_2$ **2** and the isotypic compound [Pt$_2$(mipk)$_2$(mthy)$_2$][ClO$_4$]$_2$ **3** the nucleobases show head-to-tail arrangement. The intramolecular M $\cdots$ M distances vary from 2.861(1) Å in **2** to 2.879(1) Å in **1**. By ligand-exchange reaction in aqueous media the side product [Pt(mipk)$_2$][ClO$_4$]$_2$ is formed. Proton NMR studies showed that the dinuclear complexes are not stable in aqueous solution. Oxidation of **3** and [Pt$_2$(mipk)$_2$(mura)$_2$][ClO$_4$]$_2$ **4** to platinum blues with higher-valent Pt was not observed. Presumably this is due to the competing oxidation of the low-potential mipk ligand.

Thymine as a constituent of DNA and uracil [(1*H*,3*H*)-pyrimidine-2,4-dione] as a constituent of RNA can both form dinuclear platinum and palladium complexes. Their palladium complexes are interesting with respect to their intriguing co-ordination chemistry. Wide interest particularly in their platinum co-ordination compounds was initiated in 1975 by reports from Rosenberg's group on the antitumour activity of an intensively coloured class of platinum complexes. They are derived from *cis*-[Pt(NH$_3$)$_2$(H$_2$O)$_2$]$^{2+}$ and thymine, uracil or related ligands.[1] These complexes are interesting for both their biological effects and their versatile co-ordination chemistry.[2]

In a series of investigations we have studied the syntheses and chemical properties of palladium and platinum bis(imidazole) complexes with secondary bridging ligands.[3–6] Especially the platinum complexes of chelating bis(imidazole) ligands have been shown to display significant antitumour activity.[4,7,8] In order to extend the scope of our studies and to emphasize the importance of antitumour-active platinum complexes of tertiary amine ligands we chose the unsymmetric 1-methylimidazol-2-yl pyridin-2-yl ketone (mipk), the dichloro-platinum(II) complex of which displays remarkably high cytostatic properties in preliminary *in vitro* experiments on L1210 tumour cells.[9]

In this paper we report on the syntheses of the products obtained by the reaction of the diaqua(1-methylimidazol-2-yl pyridin-2-yl ketone)-palladium(II) and -platinum(II) nitrate complexes [M(mipk)(H$_2$O)$_2$][NO$_3$]$_2$ (M = Pd or Pt) with 1-methylthymine (Hmthy) and 1-methyluracil (Hmura). X-Ray diffraction of these complexes revealed that the model nucleobases react in all cases under the chosen conditions as anionic bridging secondary ligands. They connect two of the mipk-chelated metal centres to dinuclear molecular units in the head-to-tail fashion. Crystal structures of the homodinuclear complexes [Pd$_2$(mipk)$_2$(mura)$_2$][ClO$_4$]$_2$ **1**, [Pd$_2$(mipk)$_2$-(mthy)$_2$][ClO$_4$]$_2$ **2** and [Pt$_2$(mipk)$_2$(mthy)$_2$][ClO$_4$]$_2$ **3** are presented as well as that of the mononuclear side product [Pt(mipk)$_2$][ClO$_4$]$_2$.

mipk

Hmthy R = Me
Hmura R = H
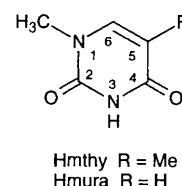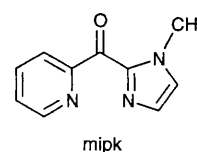
The second point we want to focus on is the solution chemistry of the nucleobase-bridged complexes containing the mipk ligand. It is remarkably different from those of the previously reported structurally analogous nucleobase-bridged Pt(bmik) compounds [bmik = bis(1-methylimidazol-2-yl) ketone].[5] This will be followed by synergistic evaluation of ^{1}H and ^{195}Pt NMR data for the dinuclear platinum complexes.

Results and Discussion

Syntheses of the complexes

The nucleobase-anion-bridged complexes [Pd$_2$(mipk)$_2$-(mura)$_2$][ClO$_4$]$_2$ **1**, [Pd$_2$(mipk)$_2$(mthy)$_2$][ClO$_4$]$_2$ **2**, [Pt$_2$-(mipk)$_2$(mthy)$_2$][ClO$_4$]$_2$ **3** and [Pt$_2$(mipk)$_2$(mura)$_2$][ClO$_4$]$_2$ **4** were formed upon treatment of 1-methylthymine or 1-methyl-uracil with an acidic aqueous solution of diaqua(1-methylimid-azol-2-yl pyridin-2-yl ketone)-palladium(II) and - platinum(II) nitrate, [M(mipk)(H$_2$O)$_2$][NO$_3$]$_2$ (M = Pd or Pt). This reaction was accompanied by a change from yellow to orange for the palladium(II) compounds and from pale orange to deep red for the platinum(II) compounds. This indicates formation of the dinuclear complexes. For compounds **1–3** this was confirmed by single-crystal X-ray diffraction analyses, which also revealed that for all the cases reported here the bridging nucleobases

Table 1 Selected interatomic distances (Å) and angles (°) for complex **1**

Pd(1)···Pd(2)	2.879(1)	N(9)–C(26)	1.392(5)	N(3)–C(9)	1.353(6)	C(7)–C(8)	1.375(7)
Pd(1)–N(8)	2.026(4)	N(9)–C(30)	1.468(6)	N(4)–C(13)	1.339(5)	C(8)–C(9)	1.374(6)
Pd(1)–O(6)	2.032(3)	N(10)–C(27)	1.357(5)	N(4)–C(11)	1.355(6)	C(11)–C(12)	1.363(6)
Pd(1)–N(3)	2.060(3)	N(10)–C(26)	1.387(5)	N(5)–C(13)	1.353(6)	C(13)–C(14)	1.467(6)
Pd(1)–N(1)	1.985(4)	O(1)–C(4)	1.219(6)	N(5)–C(12)	1.366(6)	C(14)–C(15)	1.497(7)
Pd(2)–N(4)	1.979(3)	O(2)–C(14)	1.216(5)	N(5)–C(20)	1.464(6)	C(15)–C(16)	1.392(7)
Pd(2)–O(4)	2.012(3)	O(3)–C(21)	1.222(6)	N(6)–C(19)	1.356(6)	C(16)–C(17)	1.368(9)
Pd(2)–N(6)	2.014(4)	O(4)–C(22)	1.275(6)	N(6)–C(15)	1.358(6)	C(17)–C(18)	1.369(9)
Pd(2)–N(10)	2.035(3)	O(5)–C(26)	1.218(5)	N(7)–C(24)	1.362(8)	C(18)–C(19)	1.359(7)
N(1)–C(3)	1.325(6)	O(6)–C(27)	1.272(5)	N(7)–C(21)	1.391(6)	C(22)–C(23)	1.429(6)
N(1)–C(1)	1.389(6)	C(1)–C(2)	1.356(8)	N(7)–C(25)	1.471(6)	C(23)–C(24)	1.311(9)
N(2)–C(2)	1.353(8)	C(3)–C(4)	1.470(7)	N(8)–C(22)	1.349(6)	C(27)–C(28)	1.435(5)
N(2)–C(3)	1.364(6)	C(4)–C(5)	1.497(7)	N(8)–C(21)	1.375(6)	C(28)–C(29)	1.333(6)
N(2)–C(10)	1.468(7)	C(5)–C(6)	1.385(6)	N(9)–C(29)	1.361(6)		
N(3)–C(5)	1.349(5)	C(6)–C(7)	1.370(8)				

N(1)–Pd(1)–N(8)	90.6(2)	C(26)–N(10)–Pd(2)	111.8(3)	C(3)–N(2)–C(10)	128.7(5)	C(13)–C(14)–C(15)	120.2(4)
N(1)–Pd(1)–O(6)	175.5(1)	C(22)–O(4)–Pd(2)	126.8(3)	C(5)–N(3)–C(9)	117.1(4)	N(6)–C(15)–C(16)	120.5(5)
N(8)–Pd(1)–O(6)	85.1(1)	C(27)–O(6)–Pd(1)	126.9(3)	C(5)–N(3)–Pd(1)	127.1(3)	N(6)–C(15)–C(14)	121.5(4)
N(1)–Pd(1)–N(3)	91.7(2)	C(2)–C(1)–N(1)	108.5(5)	C(9)–N(3)–Pd(1)	115.8(3)	C(16)–C(15)–C(14)	117.8(4)
N(8)–Pd(1)–N(3)	177.2(1)	N(2)–C(2)–C(1)	107.7(5)	C(13)–N(4)–C(11)	107.3(4)	C(17)–C(16)–C(15)	120.6(5)
O(6)–Pd(1)–N(3)	92.6(1)	N(1)–C(3)–N(2)	110.4(4)	C(13)–N(4)–Pd(2)	122.5(3)	C(18)–C(17)–C(16)	118.1(5)
N(1)–Pd(1)–Pd(2)	99.0(1)	N(1)–C(3)–C(4)	126.4(4)	C(11)–N(4)–Pd(2)	128.8(3)	C(19)–C(18)–C(17)	120.3(5)
N(8)–Pd(1)–Pd(2)	81.0(1)	N(2)–C(3)–C(4)	123.0(4)	C(13)–N(5)–C(12)	107.6(4)	N(6)–C(19)–C(18)	122.5(5)
O(6)–Pd(1)–Pd(2)	81.9(1)	O(1)–C(4)–C(3)	119.6(5)	C(13)–N(5)–C(20)	128.3(4)	O(3)–C(21)–N(8)	121.5(4)
N(3)–Pd(1)–Pd(2)	100.3(1)	O(1)–C(4)–C(5)	118.3(5)	C(12)–N(5)–C(20)	124.0(4)	O(3)–C(21)–N(7)	121.5(5)
N(4)–Pd(2)–O(4)	179.6(1)	C(3)–C(4)–C(5)	121.9(4)	C(19)–N(6)–C(15)	117.9(4)	N(8)–C(21)–N(7)	117.0(5)
N(4)–Pd(2)–N(6)	90.8(2)	N(3)–C(5)–C(6)	121.6(4)	C(19)–N(6)–Pd(2)	117.3(3)	O(4)–C(22)–N(8)	122.9(4)
O(4)–Pd(2)–N(6)	89.4(2)	N(3)–C(5)–C(4)	122.9(4)	C(15)–N(6)–Pd(2)	124.6(3)	O(4)–C(22)–C(23)	118.8(4)
N(4)–Pd(2)–N(10)	93.4(1)	C(6)–C(5)–C(4)	115.6(4)	C(24)–N(7)–C(21)	120.5(5)	N(8)–C(22)–C(23)	118.3(4)
O(4)–Pd(2)–N(10)	86.4(1)	C(7)–C(6)–C(5)	120.5(5)	C(24)–N(7)–C(25)	122.1(5)	C(24)–C(23)–C(22)	119.1(5)
N(6)–Pd(2)–N(10)	175.6(1)	C(6)–C(7)–C(8)	118.4(4)	C(21)–N(7)–C(25)	117.2(6)	C(23)–C(24)–N(7)	122.1(5)
N(4)–Pd(2)–Pd(1)	97.0(1)	C(7)–C(8)–C(9)	118.8(5)	C(22)–N(8)–C(21)	122.4(4)	O(5)–C(26)–N(10)	121.6(4)
O(4)–Pd(2)–Pd(1)	82.6(1)	N(3)–C(9)–C(8)	123.6(4)	C(22)–N(8)–Pd(1)	126.5(3)	O(5)–C(26)–N(9)	121.3(4)
N(6)–Pd(2)–Pd(1)	99.1(1)	N(4)–C(11)–C(12)	108.9(4)	C(21)–N(8)–Pd(1)	111.1(3)	N(10)–C(26)–N(9)	117.1(4)
N(10)–Pd(2)–Pd(1)	81.9(1)	C(11)–C(12)–N(5)	106.8(4)	C(29)–N(9)–C(26)	120.9(4)	O(6)–C(27)–N(10)	122.7(3)
C(3)–N(1)–C(1)	106.1(4)	N(4)–C(13)–N(5)	109.4(4)	C(29)–N(9)–C(30)	121.3(4)	O(6)–C(27)–C(28)	118.9(4)
C(3)–N(1)–Pd(1)	127.2(3)	N(4)–C(13)–C(14)	126.4(4)	C(26)–N(9)–C(30)	117.7(4)	N(10)–C(27)–C(28)	118.4(4)
C(1)–N(1)–Pd(1)	126.6(3)	N(5)–C(13)–C(14)	124.2(4)	C(27)–N(10)–C(26)	122.5(3)	C(29)–C(28)–C(27)	118.9(4)
C(2)–N(2)–C(3)	107.3(4)	O(2)–C(14)–C(13)	120.7(5)	C(27)–N(10)–Pd(2)	125.1(3)	C(28)–C(29)–N(9)	122.1(4)
C(2)–N(2)–C(10)	123.7(5)	O(2)–C(14)–C(15)	119.1(4)				
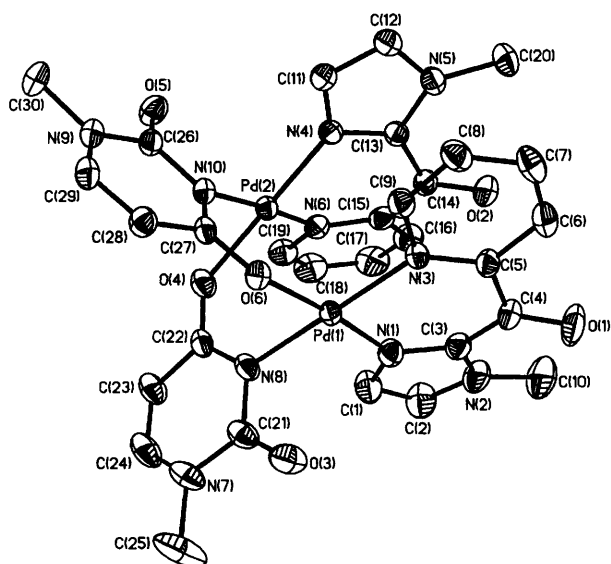
Fig. 1 Molecular cation of complex **1** with ellipsoids at the 30% probability level and atom labelling

show head-to-tail orientation. The structure of the side product [Pt(mipk)₂][ClO₄]₂ **5** which cocrystallizes in the reaction mixtures of **3** and **4** was also determined by single-crystal X-ray diffraction analysis. The chelating ligand mipk is accessible by reaction of 1-methylimidazole with butyllithium and subsequent

treatment with ethyl pyridine-2-carboxylate.[10] The elemental analyses of **1–5** are in accord with their formulas as obtained by crystal structure determination.

Crystal structure of [Pd₂(mipk)₂(mura)₂][ClO₄]₂ 1

Selected interatomic distances and angles are reported in Table 1. A thermal ellipsoid plot of the molecular cation is shown in Fig. 1. The cation is dinuclear with respect to palladium. Two of the mipk-chelated palladium atoms are bridged by 1-methyluracilate ligands through their N^3 [N(8), N(10)] and O^4 [O(4), O(6)] donor functions. The two nucleobase anions are arranged in the head-to-tail fashion, resulting in N_3O co-ordination spheres for each palladium atom. The two mipk ligands are oriented antiparallel towards each other. This can very clearly be seen in a view along the Pd···Pd axis. The methylimidazole ring of one ligand lies above the pyridine ring of the other ligand and *vice versa*, thus resulting in a molecular C_2 symmetry. This structural motif is also observed for **2** and **3**.

The intramolecular Pd···Pd distance is 2.879 Å. The two palladium atoms do not differ significantly from the best least-squares planes through their co-ordination spheres. The bite of the 1-methyluracilates [O(4)···N(8), O(6)···N(10)] is 2.31 Å. This is considerably smaller than the metal–metal distance, resulting in a dihedral angle between the two square-planar metal co-ordination planes of $\tau = 23.8°$. In addition, a mean torsion angle of $\omega = 2.2°$ is observed along the Pd···Pd vector. Complex **1** is the first crystallographically characterized example of an uracilate-bridged palladium compound.

Table 2 Selected interatomic distances (Å) and angles (°) for complex 2

Pd(1)···Pd(2)	2.861(1)	Pd(2)–N(4)	1.985(3)
Pd(1)–N(1)	1.992(3)	Pd(2)–O(4)	2.012(3)
Pd(1)–O(5)	2.010(2)	Pd(2)–N(10)	2.045(3)
Pd(1)–N(3)	2.035(3)	Pd(2)–N(6)	2.068(3)
Pd(1)–N(8)	2.043(3)		
N(1)–Pd(1)–O(5)	179.29(10)	N(4)–Pd(2)–O(4)	174.29(11)
N(1)–Pd(1)–N(3)	89.04(12)	N(4)–Pd(2)–N(10)	90.82(12)
O(5)–Pd(1)–N(3)	90.84(11)	O(4)–Pd(2)–N(10)	85.89(11)
N(1)–Pd(1)–N(8)	94.51(12)	N(4)–Pd(2)–N(6)	90.81(13)
O(5)–Pd(1)–N(8)	85.62(11)	O(4)–Pd(2)–N(6)	92.46(12)
N(3)–Pd(1)–N(8)	176.40(11)	N(10)–Pd(2)–N(6)	178.35(12)
N(1)–Pd(1)–Pd(2)	97.21(8)	N(4)–Pd(2)–Pd(1)	102.33(9)
O(5)–Pd(1)–Pd(2)	82.11(7)	O(4)–Pd(2)–Pd(1)	81.83(7)
N(3)–Pd(1)–Pd(2)	98.33(9)	N(10)–Pd(2)–Pd(1)	81.58(8)
N(8)–Pd(1)–Pd(2)	81.84(8)	N(6)–Pd(2)–Pd(1)	98.32(8)

Table 3 Selected interatomic distances (Å) and angles (°) for complex 3

Pt(1)···Pt(2)	2.871(1)	Pt(2)–N(4)	1.985(9)
Pt(1)–N(3)	2.025(9)	Pt(2)–O(4)	2.030(7)
Pt(1)–O(5)	2.029(6)	Pt(2)–N(10)	2.046(8)
Pt(1)–N(8)	2.049(8)	Pt(2)–N(6)	2.064(8)
Pt(1)–N(1)	1.987(8)		
N(1)–Pt(1)–N(3)	89.4(3)	N(4)–Pt(2)–O(4)	173.9(3)
N(1)–Pt(1)–O(5)	179.6(3)	N(4)–Pt(2)–N(10)	91.7(4)
N(3)–Pt(1)–O(5)	91.0(3)	O(4)–Pt(2)–N(10)	84.8(3)
N(1)–Pt(1)–N(8)	94.8(3)	N(4)–Pt(2)–N(6)	90.5(4)
N(3)–Pt(1)–N(8)	175.7(3)	O(4)–Pt(2)–N(6)	93.0(3)
O(5)–Pt(1)–N(8)	84.8(3)	N(10)–Pt(2)–N(6)	177.8(3)
N(1)–Pt(1)–Pt(2)	98.6(2)	N(4)–Pt(2)–Pt(1)	104.2(2)
N(3)–Pt(1)–Pt(2)	96.8(2)	O(4)–Pt(2)–Pt(1)	80.4(2)
O(5)–Pt(1)–Pt(2)	81.3(2)	N(10)–Pt(2)–Pt(1)	82.9(2)
N(8)–Pt(1)–Pt(2)	83.6(2)	N(6)–Pt(2)–Pt(1)	96.7(2)

Compared to the analogous platinum compound cis-[Pt$_2$-(NH$_3$)$_4$(mura)$_2$][NO$_3$]$_2$·3H$_2$O (head-to-tail)[11] the metal–metal distance in **1** is shorter. This is in contrast to [Pt$_2$(bmik)$_2$-(mura)$_2$][NO$_3$]$_2$·2H$_2$O (head-to-tail) where the Pt···Pt distance is slightly shorter than in **1**. An overview of the related compounds characterized crystallographically is given in Table 5.

Interesting features of the complexes are the relatively large dihedral angles between the best least-squares planes through the 1-methylimidazole ring and the pyridine ring of the mipk ligands. They are ψ[Pd(1)] = 14.8° and ψ[Pd(2)] = 27.5°. This represents a remarkable difference from planarity as might not be expected for the mipk ligand, as it contains an sp^2-hybridized C$_1$-ketone bridge between the two heterocyclic rings. The bonding distances and angles of both crystallographically independent ligands are in the same range and are well within the expected values. The mura bases are almost planar with the exocyclic metal-co-ordinated O(4) atom showing the most significant deviation (0.09 Å) from the best plane through the pyrimidine ring system. The bonding distances and angles lie within previously reported values.
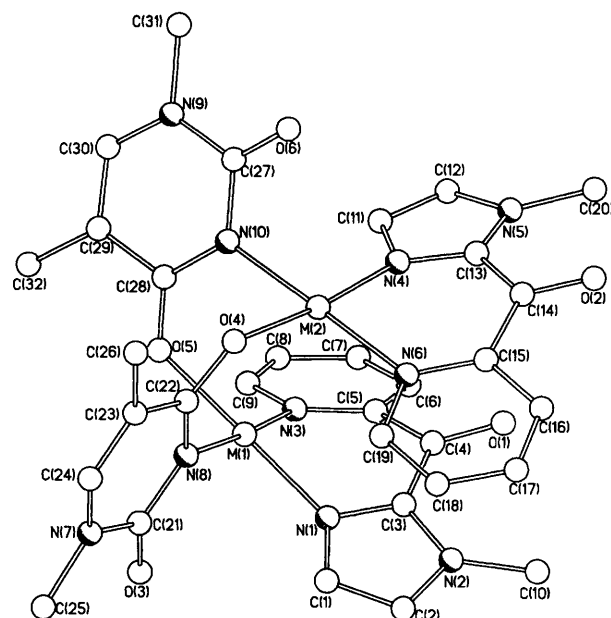
The shortest intermolecular distance between two dinuclear cations amounts to 5.251 Å [Pd(2)···Pd(2a); a −x, 1 − y, 1 − z] in a range where intermetallic interaction can be neglected. Furthermore the two crystallographically independent perchlorate anions are loosely fixed in the unit cell. Since water molecules could not be detected in the Fourier-difference maps and the molecular cation does not have any donor atoms, no hydrogen-bonding interaction is observed in the crystal structure of **1**.

Crystal structures of [Pd$_2$(mipk)$_2$(mthy)$_2$][ClO$_4$]$_2$ 2 and [Pt$_2$(mipk)$_2$(mthy)$_2$][ClO$_4$]$_2$ 3

Compounds **2** and **3** crystallize isotypically in the triclinic crystal system in the space group $P\bar{1}$. The unit cells contain two dinuclear cations and four perchlorate anions. A perspective view of the structure of the cation of **2** and **3** is depicted in Fig. 2. Selected interatomic distances and angles are given in Tables 2 and 3 for **2** and **3**, respectively. Two mipk-chelated metal moieties are bridged by two 1-methylthyminate ligands. The nucleobase anions show head-to-tail arrangement and the two mipk ligands are oriented antiparallel, too. Thus, the cations are generally similar to the 1-methyluracilato complex described above. There are, however, some significant differences. The N–O bite distances of 2.30 Å [O(4)···N(8) and O(5)···N(10)] in **2** and 2.32 [O(4)···N(8)] and 2.33 Å [O(5)···N(10)] in **3** are comparable to the value of 2.31 Å in **1**. Furthermore the metal–metal distances lie essentially in the same range. Values of 2.861 and 2.871 Å are observed for **2** and **3**, respectively. Besides the two head-to-head 1-methyl-thyminato-bridged complexes [Pd$_2$(bipy)$_2$(mthy)$_2$][NO$_3$]$_2$·

Fig. 2 Structure of the cations of complexes **2** and **3** with atom labelling (M = Pd or Pt)

5.5H$_2$O (bipy = 2,2′-bipyridine) (Pd···Pd 2.848 Å)[12] and cis-[(H$_3$N)$_2$Pt(mthy)$_2$PtCl$_2$]·3H$_2$O (Pd···Pd 2.861 Å),[13] they are to our knowledge the shortest values for head-to-tail 1-methylthyminato-bridged complexes found so far. The dihedral angles between the two square-planar co-ordination spheres of each cation are τ = 24.0° in both complexes, while the torsion angles differ slightly with ω = 8.5° in **2** and 9.1° in **3** compared to the rather small value of 2.2° in **1**. The bonding distances and angles of the two crystallographically independent mipk ligands of each cation, as well as in comparison to those of the isotypical structure, show no unusual values. The large angles observed between the two heterocyclic rings of one ligand are remarkable. They are ψ[Pd(1)] = 30.0° and ψ[Pd(2)] = 20.8° in **2** and ψ[Pt(1)] = 29.9° and ψ[Pt(2)] = 22.7° in **3**. The steric tensions they cause may be the reason for the instability of these complexes in aqueous solution as described below. In contrast the structurally analogous compounds [Pt$_2$(bmik)$_2$-(mura)$_2$][NO$_3$]$_2$·2H$_2$O {ψ[Pt(1)] = 12°} and [Pt$_2$(bmik)$_2$-(mthy)$_2$][ClO$_4$]$_2$·5H$_2$O {ψ[Pt(1)] = 11, ψ[Pt(2)] = 12°} are stable upon dissolution.[5]

The shortest distances between two metal atoms of two adjacent cations are 5.687 Å in complex **2** and 5.660 Å in **3** [M(1)···M(1a), M = Pd or Pt; a −x, −y, 1 − z]. A tendency to build tetrameric cations is not observed for the dinuclear units as in the crystal structure of the 1-methylthyminate-
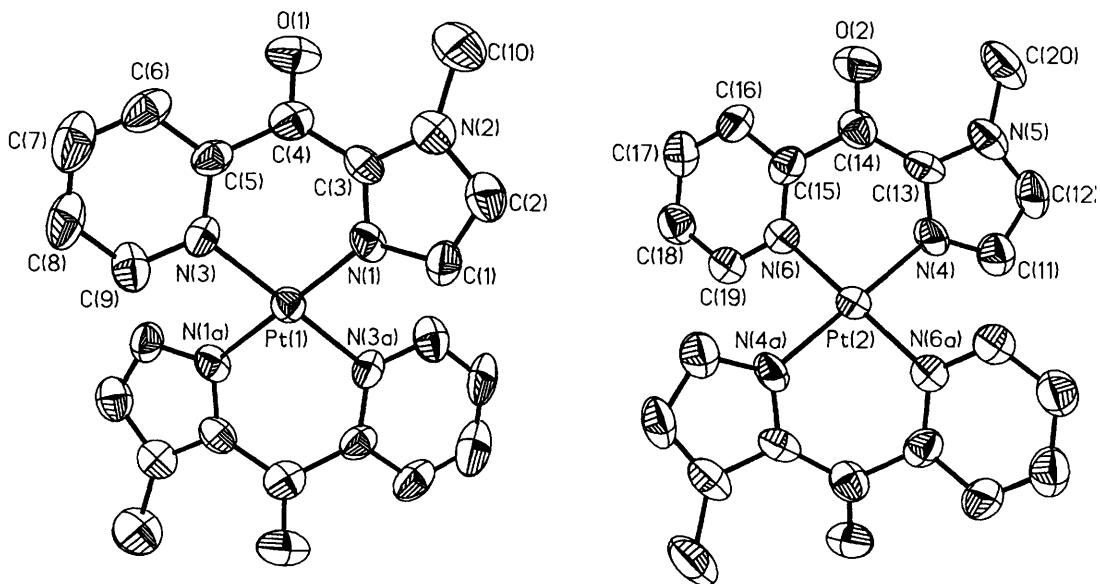
Fig. 3 Structure of the molecular cations of complex **5** with ellipsoids at the 50% probability level
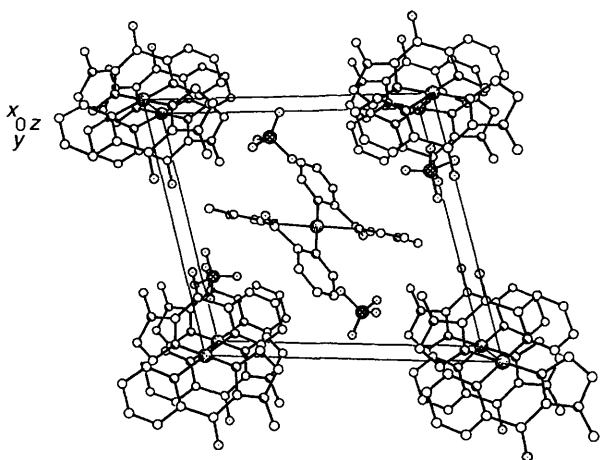

Fig. 4 Unit cell of complex **5** viewed along the x-axis

bridged complex cis-[Pt$_2$(NH$_3$)$_4$(mthy)$_2$][NO$_3$]$_2$,[22] where hydrogen bonding occurs between the exocyclic O^2 sites of one cation with the two NH$_3$ groups of the adjacent cation, forming infinite strands. The reasons are the same as mentioned for the complexes [Pt$_2$(bmik)$_2$(mura)$_2$][NO$_3$]$_2$·2H$_2$O and [Pt$_2$(bmik)$_2$(mthy)$_2$][ClO$_4$]$_2$·5H$_2$O.[5] Since the chelating ligands are tertiary amines there is no possibility of the formation of hydrogen bonds between the molecular cations for these compounds. This allows a more flexible arrangement of the dinuclear cations with long intermolecular metal–metal distances. As in **2** and **3** crystal water molecules could not be detected, no hydrogen bonding is observed.

Crystal structure of [Pt(mipk)$_2$][ClO$_4$]$_2$ **5**

Fig. 3 shows thermal ellipsoid plots of the two crystallographically independent molecular cations of complex **5**. Selected interatomic distances and angles are given in Table 4. The asymmetric unit contains two half cations with the platinum atoms lying on inversion centres, and two perchlorate anions. Two mipk ligands co-ordinate via their free nitrogen-donor atoms to one central platinum atom, thus resulting in a square-planar PtN$_4$ co-ordination sphere. The six-membered chelate rings [Pt(1), N(1), C(3), C(4), C(5), N(3) and Pt(2), N(4), C(13), C(14), C(15), N(6)] both show boat configurations. The bonding distances and angles within the mipk ligands lie in the same range as for the compounds reported above. Remarkable

are the very large angles between the two heterocyclic rings of the ligands. They are nearly identical, ψ[Pt(1)] = 47.2° and ψ[Pt(2)] = 47.1°. In Fig. 4 a plot of the unit cell of **5** is depicted. The shortest intermolecular Pt · · · Pt distance is 7.998 Å and corresponds to one translation in direction of the x axis. The distance between the two crystallographically independent platinum atoms in the unit cell is 11.64 Å in a range where metal–metal interaction is impossible. Hydrogen-bonding interactions are not observed. This compound is very interesting because it cocrystallizes in the reaction mixtures of **3** and **4**. Thus the formation of **5** can only be explained by ligand-exchange reactions in the aqueous medium. This is of considerable importance with respect to the solution behaviour of the dinuclear nucleobase-anion-bridged compounds.

Solution behaviour of complexes 1–4

Dissolving the pure crystalline nucleobase-bridged complexes in D$_2$O–(CD$_3$)$_2$CO leads to formation of a mixture of several mono- and di-nuclear species as observed in the ^{1}H NMR spectra. The dinuclear ones are the original head-to-tail-bridged compounds and the μ-hydroxo-bridged species [(mipk)Pt(μ-OH)$_2$Pt(mipk)]$^{2+}$. There is no indication that head-to-head nucleobase-bridged complexes exist in solution. This is very different from the solution chemistry of α-pyridonate-bridged cis-[Pt(NH$_3$)$_2$]$^{2+}$ and [Pt(en)]$^{2+}$ (en = ethane-1,2-diamine) moieties, where a head-to-tail to head-to-head isomerization in solution has been observed.[23] Mononuclear compounds detected by NMR spectroscopy are [Pt(mipk)(H$_2$O)L]$^+$, [Pt(H$_2$O)$_2$L$_2$] (L = mura or mthy) and [Pt(mipk)$_2$][ClO$_4$]$_2$ **5**, which cocrystallizes in the reaction mixtures of **3** and **4**. Additionally, ^{1}H NMR signals of free Hmthy and Hmura were detected. The signals of the bridging nucleobases and chelating ligands assigned by their intensity and their characteristic chemical shift in comparison to those of analogous co-ordination compounds are given in Table 6. The ^{1}H NMR spectra display very clearly that the dinuclear compounds are not stable upon dissolving in D$_2$O–(CD$_3$)$_2$CO. Besides the expected resonance signals of the methyl groups there are some more less-intense signals. The same occurs in the aromatic region of the spectra; therefore an unambiguous assignment of the pyridine-ring protons is not possible due to overlapping groups of signals.

To get more insight and a better understanding of what happens when the pure crystalline dinuclear complexes are dissolved in D$_2$O–(CD$_3$)$_2$CO$_6$, ^{195}Pt NMR spectra were recorded of reaction mixtures of **3** and **4** in D$_2$O (see Fig. 5). The

Table 4 Selected interatomic distances (Å) and angles (°) for complex **5**. Symmetry transformations: ^{a} $-x + 1$, $-y + 1$, $-z + 1$; ^{b} $-x$, $-y$, $-z$

Pt(1)–N(1)	2.008(6)	N(5)–C(20)	1.459(13)	N(2)–C(2)	1.409(13)	C(8)–C(9)	1.366(15)
Pt(1)–N(3)	2.039(6)	N(6)–C(19)	1.343(13)	N(2)–C(10)	1.467(14)	C(11)–C(12)	1.362(14)
Pt(2)–N(4)	2.030(7)	N(6)–C(15)	1.339(11)	N(3)–C(9)	1.333(12)	C(13)–C(14)	1.433(15)
Pt(2)–N(6)	2.028(7)	C(1)–C(2)	1.318(13)	N(3)–C(5)	1.354(11)	C(14)–C(15)	1.513(14)
O(1)–C(4)	1.221(11)	C(3)–C(4)	1.480(13)	N(4)–C(13)	1.311(11)	C(15)–C(16)	1.394(13)
O(2)–C(14)	1.232(13)	C(4)–C(5)	1.495(13)	N(4)–C(11)	1.336(12)	C(16)–C(17)	1.341(15)
N(1)–C(3)	1.314(12)	C(5)–C(6)	1.391(12)	N(5)–C(12)	1.373(14)	C(17)–C(18)	1.376(15)
N(1)–C(1)	1.375(11)	C(6)–C(7)	1.318(17)	N(5)–C(13)	1.384(12)	C(18)–C(19)	1.385(15)
N(2)–C(3)	1.345(11)	C(7)–C(8)	1.318(19)				
N(1)–Pt(1)–N(1a)^a	180.0	C(1)–C(2)–N(2)	106.8(9)	C(2)–N(2)–C(10)	123.4(9)	C(11)–C(12)–N(5)	107.0(9)
N(1)–Pt(1)–N(3a)^a	92.9(3)	N(1)–C(3)–N(2)	110.2(8)	C(9)–N(3)–C(5)	118.9(8)	N(4)–C(13)–N(5)	107.6(9)
N(1)–Pt(1)–N(3)	87.1(3)	N(1)–C(3)–C(4)	124.8(7)	C(9)–N(3)–Pt(1)	119.6(7)	N(4)–C(13)–C(14)	125.1(9)
N(1a)^a–Pt(1)–N(3)	92.9(3)	N(2)–C(3)–C(4)	124.7(8)	C(5)–N(3)–Pt(1)	121.4(6)	N(5)–C(13)–C(14)	127.0(9)
N(3a)^a–Pt(1)–N(3)	180.0	O(1)–C(4)–C(5)	119.3(9)	C(13)–N(4)–C(11)	110.5(8)	O(2)–C(14)–C(13)	121.9(10)
N(4a)^b–Pt(2)–N(4)	180.0	O(1)–C(4)–C(3)	123.7(9)	C(13)–N(4)–Pt(2)	120.7(6)	O(2)–C(14)–C(15)	119.8(10)
N(4a)^b–Pt(2)–N(6)	93.9(3)	C(5)–C(4)–C(3)	116.4(8)	C(11)–N(4)–Pt(2)	128.4(7)	C(13)–C(14)–C(15)	117.8(8)
N(4)–Pt(2)–N(6)	86.1(3)	N(3)–C(5)–C(6)	118.4(9)	C(12)–N(5)–C(13)	106.9(8)	N(6)–C(15)–C(16)	120.9(9)
N(4)–Pt(2)–N(6a)^b	93.9(3)	N(3)–C(5)–C(4)	122.5(8)	C(12)–N(5)–C(20)	126.8(9)	N(6)–C(15)–C(14)	121.5(8)
N(6)–Pt(2)–N(6a)^b	180.0	C(6)–C(5)–C(4)	118.7(8)	C(13)–N(5)–C(20)	126.2(10)	C(16)–C(15)–C(14)	116.6(9)
C(3)–N(1)–C(1)	107.3(7)	C(7)–C(6)–C(5)	121.7(11)	C(19)–N(6)–C(15)	120.4(8)	C(17)–C(16)–C(15)	118.5(10)
C(3)–N(1)–Pt(1)	121.4(6)	C(8)–C(7)–C(6)	119.3(11)	C(19)–N(6)–Pt(2)	118.4(7)	C(16)–C(17)–C(18)	121.2(10)
C(1)–N(1)–Pt(1)	130.4(6)	C(7)–C(8)–C(9)	120.7(12)	C(15)–N(6)–Pt(2)	120.8(6)	C(17)–C(18)–C(19)	118.6(10)
C(3)–N(2)–C(2)	106.3(8)	N(3)–C(9)–C(8)	121.1(11)	C(2)–C(1)–N(1)	109.4(9)	N(6)–C(19)–C(18)	120.4(10)
C(3)–N(2)–C(10)	130.4(10)	N(4)–C(11)–C(12)	107.9(10)				

Table 5 Structural details of homonuclear mthy- and mura-bridged complexes of Pd^{II} and Pt^{II} $d_{M\cdots M}$ = intramolecular metal–metal distance, τ = dihedral angle between two adjacent metal co-ordination planes of one dimeric unit, ω = torsion angle along the M $\cdots$ M vector, h.t. = head-to-tail, h.h. = head-to-head, t.w. = this work

Compound	Isomer	$d_{M\cdots M}$/Å	τ/°	ω/°	Ref.
1 [Pd$_2$(mipk)$_2$(mura)$_2$][ClO$_4$]$_2$	h.t.	2.879	23.8	2.2	t.w.
cis-[Pt$_2$(NH$_3$)$_4$(mura)$_2$][NO$_3$]$_2$·3H$_2$O	h.t.	2.954	35.8	19.2	14
[Pt$_2$(bmik)$_2$(mura)$_2$][NO$_3$]$_2$·2H$_2$O	h.t.	2.841	25	25	5
cis-[Pt$_2$(NH$_3$)$_4$(mura)$_2$][NO$_3$]$_2$·H$_2$O	h.h.	2.937	34.1	25.2	15
cis-[(H$_3$N)$_2$Pt(mura)$_2$Pt(bipy)][NO$_3$]$_2$·3H$_2$O	h.h.	2.929	30.4	10.2	16
2 [Pd$_2$(mipk)$_2$(mthy)$_2$][ClO$_4$]$_2$	h.t	2.861	24.0	8.5	t.w.
3 [Pt$_2$(mipk)$_2$(mthy)$_2$][ClO$_4$]$_2$	h.t	2.871	24.0	9.1	t.w.
[Pt$_2$(bmik)$_2$(mthy)$_2$][NO$_3$]$_2$·5H$_2$O	h.t	2.900	11	23	5
[Pt$_2$(dmbi)$_2$(mthy)$_2$][ClO$_4$]$_2$·4H$_2$O^a	h.t	2.848	23	4	17
cis-[Pt$_2$(NH$_3$)$_4$(mthy)$_2$][NO$_3$]$_2$·H$_2$O	h.t	2.974	36.1	13.8	18
cis-[Pt$_2$(NH$_3$)$_4$(mthy)$_2$][NO$_3$]$_2$·4.5H$_2$O^b	h.t	2.920	35.2	25.7	19
		2.915	30.7	17.9	
[Pd$_2$(bipy)$_2$(mthy)$_2$][NO$_3$]$_2$·5.5H$_2$O	h.h.	2.848	15.8	—	12
cis-[Pt$_2$(NH$_3$)$_4$(mthy)$_2$][NO$_3$]$_2$	h.h.	2.927	31.4	1.9	20
cis-[Pt$_2$(NH$_3$)$_4$(mthy)$_2$][NO$_3$]$_2$	h.h.	2.909	29.5	1.1	21
cis-[(H$_3$N)$_2$Pt(mthy)$_2$Pt(NH$_3$)Cl][Pt(NH$_3$)Cl$_3$]·H$_2$O	h.h.	2.939	31.5	0.8	13
cis-[(H$_3$N)$_2$Pt(mthy)$_2$PtCl$_2$]·3H$_2$O	h.h.	2.861	22.5	3.0	13

^{a} dmbi = 1,1′-dimethyl-2,2′-bis(imidazole). ^{b} Data for the two crystallographically independent cations in the asymmetric unit.

^{1}H NMR spectra of these samples essentially proved to be identical with those of the dissolved crystals. Additionally, a sample containing only the [Pt(mipk)Cl$_2$] complex and silver nitrate was measured to facilitate the assignment of species in solution without any nucleobase co-ordination (sample 1). This spectrum displays a large peak at δ -2364 assigned to [Pt(mipk)$_2$]$^{2+}$ and a small peak at δ -2097 assigned to [Pt-(mipk)(H$_2$O)$_2$]$^{2+}$. In a freshly prepared solution the inversed intensities would be expected. The diaqua complex decomposes due to ligand rearrangements into the kinetically rather inert bis(mipk) complex and free mipk. When a nucleobase is added the large peak remains, whereas the small peak disappears upon reaction. A complete analysis of the ^{195}Pt NMR spectra is given in Table 7. The pH dependence of the ^{195}Pt NMR spectrum of the diaqua complex was not studied.

The most likely reactions taking place when complexes **3** and **4** are dissolved are depicted in Scheme 1. The dinuclear cations most probably are hydrolysed to two mononuclear species (step a), which themselves may turn into a µ-hydroxo-bridged species

and the free nucleobases (step b), or into two mononuclear species (step c). There are several reasons to postulate these suggested ligand rearrangements. In accordance with the five postulated platinum adducts, also five dominant platinum species were observed in the ^{195}Pt NMR spectra. The characteristic ^{1}H NMR resonance signals of the free nucleobases forming in step b were detected in the spectra of **3** and **4**. The existence of **5** forming in step c was proven by isolation of the complex from the reaction mixtures of **3** and **4** and by subsequent characterization by X-ray diffraction analysis.
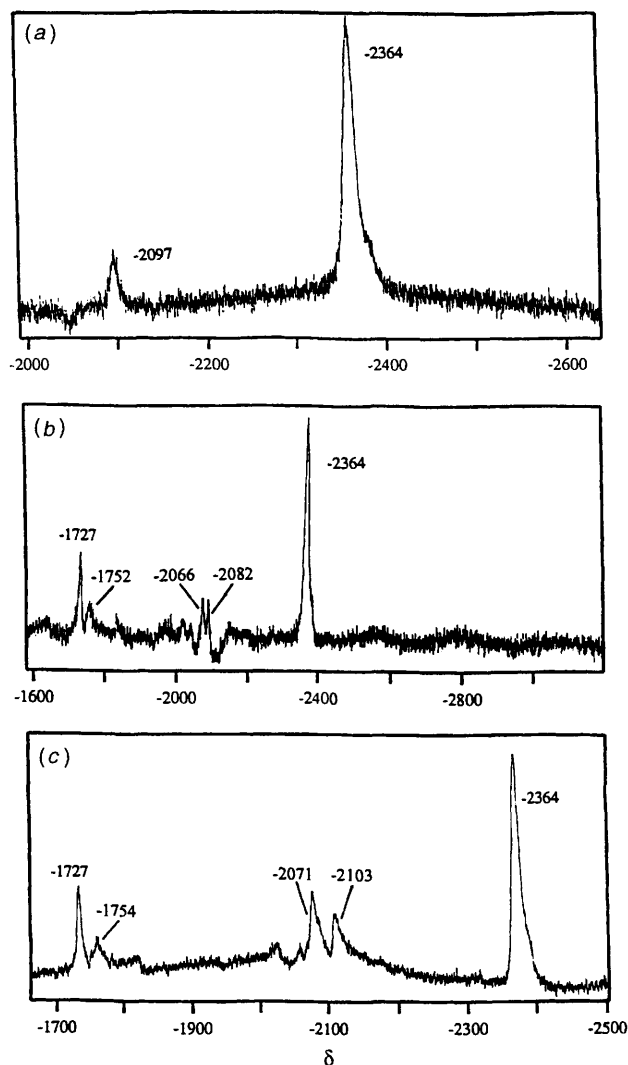
Experimental

Materials and methods

All reagents were obtained from commercial sources and used without further purification. Elemental analyses as well as the NMR spectra which were recorded on Bruker WH 300 (^{1}H,

Table 6 Proton NMR data (δ) for complexes 1–5

Compound	H^6 of mura or mthy	H^5 of mura	N(1)–CH$_3$	C(5)–CH$_3$	N$_{mipk/bmik}$–CH$_3$	Imidazole protons	Ref.
Hmthy	7.45	—	3.33	1.86	—	—	12
3 [Pt$_2$(mipk)$_2$(mthy)$_2$][ClO$_4$]$_2$	7.49	—	3.44	1.92	3.82	7.41, 6.55	t.w.
2 [Pd$_2$(mipk)$_2$(mthy)$_2$][ClO$_4$]$_2$	7.52	—	3.48	1.93	3.88	7.41, 6.55	t.w.
[Pt$_2$(bmik)$_2$(mthy)$_2$[NO$_3$]$_2$	7.68	—	3.35	1.87	4.18, 4.02	7.56, 7.47 6.96, 6.84	5
Hmura	7.60	5.78	3.36	—	—	—	12
4 [Pt$_2$(mipk)$_2$(mura)$_2$][ClO$_4$]$_2$	7.66	6.17	3.49	—	3.83	7.44, 6.61	t.w.
1 [Pd$_2$(mipk)$_2$(mura)$_2$][ClO$_4$]$_2$	7.64	6.05	3.46	—	3.79	7.37, 6.46	t.w.
[Pt$_2$(bmik)$_2$(mura)$_2$][NO$_3$]$_2$	7.69	6.19	3.50	—	4.12, 4.07	7.55, 7.49 7.17, 6.71	5
5 [Pt(mipk)$_2$][ClO$_4$]$_2$	—	—	—	—	4.13	7.69, 6.85	t.w.

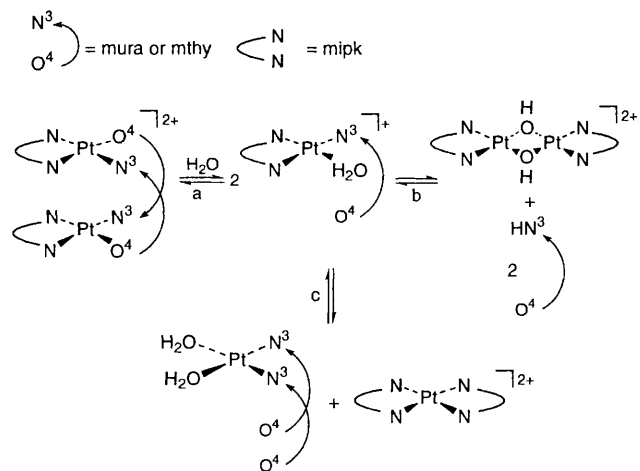**Fig. 5** The ^{195}Pt NMR spectra of (a) sample 1; [Pt(mipk)Cl$_2$] + 2 equivalents AgNO$_3$, (b) sample 2, [Pt(mipk)Cl$_2$] + 2 equivalents AgNO$_3$ + 1 equivalent Hmura and (c) sample 3, [Pt(mipk)Cl$_2$] + 2 equivalents AgNO$_3$ + 1 equivalent Hmthy

Table 7 Observed ^{195}Pt NMR signals

Sample	δ	Assignment	Co-ordination sphere
1	−2364	[Pt(mipk)$_2$]$^{2+}$	PtN$_4$
	−2097	[Pt(mipk)(H$_2$O)$_2$]$^{2+}$	PtN$_2$O$_2$
2	−2364	[Pt(mipk)$_2$]$^{2+}$	PtN$_4$
	−2082	[Pt$_2$(mipk)$_2$(mura)$_2$]$^{2+}$	PtN$_3$O
	−2066	[Pt(mipk)(mura)(H$_2$O)]$^+$	PtN$_2$O$_2$
	−1752	[Pt(mura)$_2$(H$_2$O)$_2$]	PtN$_2$O$_2$
	−1727	[(mipk)Pt(μ-OH)$_2$Pt(mipk)]$^{2+}$	
3	−2364	[Pt(mipk)$_2$]$^{2+}$	PtN$_4$
	−2103	[Pt$_2$(mipk)$_2$(mthy)$_2$]$^{2+}$	PtN$_3$O
	−2071	[Pt(mipk)(mthy)(H$_2$O)]$^+$	
	−1754	[Pt(mthy)$_2$(H$_2$O)$_2$]	PtN$_2$O$_2$
	−1727	[(mipk)Pt(μ-OH)$_2$Pt(mipk)]$^{2+}$	PtN$_2$O$_2$

Scheme 1 Species detected upon dissolving the dinuclear platinum complexes

3-trimethylsilylpropanesulfonate as internal reference) and WH 360 instruments (^{195}Pt, 77.4 MHz, pulse widths 15 Hz, saturated solution of K$_2$[PtCl$_4$] as external reference set at δ −1624, 303 K, not proton decoupled) were performed at the Institute of Organic Chemistry, University of Münster. The samples for the ^{195}Pt NMR spectra were prepared as 0.16 mol dm^{-3} (Pt) solutions by simultaneous reaction of [Pt(mipk)Cl$_2$] with 2 equivalents of AgNO$_3$ (sample 1), sample 1 and 1 equivalent of Hmura (sample 2), and sample 1 and 1 equivalent

of Hmthy (sample 3) in D$_2$O in the dark. After removal of precipitated AgCl the pH was adjusted to 1.8 in all samples without correction for deuterium isotope effects. Measurements were made 1 week after preparation to ensure that equilibria had been established.

Syntheses

1-Methylimidazol-2-yl pyridine-2-yl ketone (mipk) was prepared from 1-methylimidazole and ethyl pyridine-2-carboxylate by reaction with butyllithium as described elsewhere.[10]

Dichloro(1-methylimidazol-2-yl pyridine-2-yl ketone)plat-inum(II) [Pt(mipk)Cl$_2$], the starting material, was prepared by stirring K$_2$[PtCl$_4$] (1 mmol, 0.415 g) and mipk (1 mmol, 0.187 g) for 2 h in warm (60 °C) water (50 cm^3). The resulting

Table 8 Crystallographic data and experimental details

	1	2	3	5
Formula	$C_{30}H_{28}Cl_2N_{10}O_{14}Pd_2$	$C_{32}H_{32}Cl_2N_{10}O_{14}Pd_2$	$C_{32}H_{32}Cl_2N_{10}O_{14}Pd_2$	$C_{20}H_{18}Cl_2N_6O_{10}Pt$
M	1036.32	1064.38	1241.76	768.39
Crystal system	Triclinic	Triclinic	Triclinic	Triclinic
Space group	$P\bar{1}$	$P\bar{1}$	$P\bar{1}$	$P\bar{1}$
$a/Å$	12.891(5)	11.320(3)	11.203(2)	7.998(2)
$b/Å$	13.823(5)	13.636(4)	13.532(3)	12.170(2)
$c/Å$	13.984(5)	14.258(4)	14.196(2)	13.383(3)
$\alpha/°$	61.10(2)	88.78(3)	89.77(1)	75.19(3)
$\beta/°$	65.72(3)	83.81(2)	83.28(1)	76.26(3)
$\gamma/°$	65.10(3)	65.51(2)	66.08(1)	85.20(3)
$U/Å^3$	1910	1991	1952	1223
2θ range/°	4–54	4–54	4–54	—
Lattice segment	$+h, \pm k, \pm l$	$+h, \pm k, \pm l$	$+h, \pm k, \pm l$	$\pm h, \pm k, \pm l$
Z	2	2	2	2
T/K	293(2)	293(2)	170(2)	293(2)
$D_c/g\ cm^{-3}$	1.80	1.78	2.11	2.09
$F(000)$	1032	1064	1192	744
Crystal size/mm	0.22 × 0.34 × 0.24	0.22 × 0.25 × 0.13	0.10 × 0.02 × 0.10	Not measured
Crystal shape and colour	Yellow-orange cuboids	Orange cuboids	Deep red plates	Yellow cubes
μ/mm^{-1}	1.16	1.12	7.34	6.03
Absorption correction	ψ-Scan, empirical ^{a}	ψ-Scan, empirical ^{a}	ψ-Scan, empirical ^{a}	Combined absorption and decay correction ^{b}
Maximum, minimum transmission factors	0.775, 0.674	0.865, 0.756	0.863, 0.480	—
Unique data	8321	8735	8553	5267
Observed data [$I > 2\sigma(I)$]	7048	7286	6079	4032
Number of parameters	527	547	547	356
$R1$ [$I > 2\sigma(I)$], $wR2$ (all data) ^{c}	0.0450, 0.1302	0.0363, 0.1057	0.0475, 0.1447	0.0626, 0.1916
Weighting scheme a, b ^{d}	0.0758, 2.8915	0.0610, 1.5792	0.0381, 24.6974	0.0842, 4.6482

^{a} XEMP.^{17} ^{b} DECAY.^{24} ^{c} $R1 = \Sigma||F_o| - |F_c||/\Sigma|F_o|$, $wR2 = [\Sigma w(F_o^2 - F_c^2)^2/\Sigma w(F_o^2)^2]^{\frac{1}{2}}$. ^{d} $w = 1/[\sigma^2(F_o^2) + (aP)^2 + bP]$ where $P = [\max(F_o^2$ or 0) $+ 2F_c^2]/3$.

[Pt(mipk)Cl$_2$] was removed after cooling to 0 °C. Yield 0.404 g (0.89 mmol, 89%) of orange powder after drying.

Dichloro(1-methylimidazol-2-yl pyridine-2-yl ketone)palladium(II) [Pd(mipk)Cl$_2$] was prepared by stirring K$_2$[PdCl$_4$] (1 mmol, 0.326 g) and mipk (1 mmol, 0.187 g) in water (50 cm^3) at room temperature. After cooling to 0 °C the resulting [Pd(mipk)Cl$_2$] was filtered off. Yield 0.326 g (0.90 mmol, 90%) of beige powder after drying.

The dinuclear palladium compounds were prepared by stirring [Pd(mipk)Cl$_2$] (0.50 mmol, 0.182 g) with 2 equivalents of AgNO$_3$ (1 mmol, 0.169 g) for 2 h in water (10 cm^3) at room temperature and subsequent removal of AgCl by centrifugation, followed by addition of 49 mg (0.35 mmol) of 1-methyluracil or 44 mg (0.35 mmol) of 1-methylthymine to the freshly prepared solution of [Pd(mipk)(H$_2$O)$_2$][NO$_3$]$_2$. After 24 h at 40 °C a 0.5 mol dm^{-3} NaClO$_4$ solution (1 cm^3) was added to the warm reaction mixtures. After cooling to room temperature the filtered solutions were allowed to evaporate in the air. The platinum compounds were prepared in the same way except that [Pt(mipk)Cl$_2$] (0.50 mmol, 0.227 g) was allowed to react with 2 equivalents of AgNO$_3$ (1 mmol, 0.169 g) at 50 °C for 20 h.

[Pd$_2$(mipk)$_2$(mura)$_2$][ClO$_4$]$_2$ 1. Yellow-orange prismatic crystals of complex **1** were collected 2 d after addition of the NaClO$_4$ solution. A second batch was obtained upon further evaporation of the filtrate, providing a total yield of 54% (Found: C, 34.45; H, 2.80; N, 13.30. C$_{30}$H$_{28}$Cl$_2$N$_{10}$O$_{14}$Pd$_2$ requires C, 34.75; H, 2.70; N, 13.55%).

[Pd$_2$(mipk)$_2$(mthy)$_2$][ClO$_4$]$_2$ 2. Yellow-orange brick-shaped crystals of complex **2** were collected 1 week after addition of the NaClO$_4$ solution. A second batch was obtained from further evaporation of the filtrate, providing a total yield of 47% (Found: C, 35.55; H, 3.15; N, 12.85. C$_{32}$H$_{32}$Cl$_2$N$_{10}$O$_{14}$Pd$_2$ requires C, 36.00; H, 3.05; N, 13.15%).

[Pt$_2$(mipk)$_2$(mthy)$_2$][ClO$_4$]$_2$ 3. Deep red plates of complex **3** were collected 1–2 d after addition of the NaClO$_4$ solution. A second batch was obtained from further evaporation of the filtrate, providing a total yield of 42% (Found: C, 31.25; H, 2.65; N, 11.25. C$_{32}$H$_{32}$Cl$_2$N$_{10}$O$_{14}$Pt$_2$ requires C, 30.95; H, 2.60; N, 11.30%).

[Pt$_2$(mipk)$_2$(mura)$_2$][ClO$_4$]$_2$ 4. Deep red needles of complex **4** unfortunately not suitable for X-ray diffraction analysis were collected 1–2 d after addition of the NaClO$_4$ solution. A second batch was obtained by further evaporation of the filtrate, providing a total yield of 63% (Found: C, 29.25; H, 2.45; N, 10.90. C$_{30}$H$_{28}$Cl$_2$N$_{10}$O$_{14}$Pt$_2$ requires C, 29.70; H, 2.35; N, 11.55%).

[Pt(mipk)$_2$][ClO$_4$]$_2$ 5. Complex **5** is a side product formed in the reaction mixtures of **3** and **4**. Big yellow brick-shaped crystals of it were collected 3–4 weeks after addition of the NaClO$_4$ solution to the reaction mixture of **3** in 14% yield (Found: C, 31.00; H, 2.40; N, 10.85. C$_{20}$H$_{18}$Cl$_2$N$_6$O$_{10}$Pt requires C, 31.25; H, 2.35; N, 10.95%).

Crystallography

Intensity data were collected on a Siemens P3 diffractometer (complexes **1–3**) (Mo-Kα radiation, $\lambda = 0.710\ 73$ Å, graphite monochromator) by using the ω-scan technique and a variable scan rate (2–29° min^{-1}) and on a STOE imaging-plate diffraction system (**5**) (same radiation, etc.) with a sample-to-plate distance of 60 mm and a scan range from 0 to 180° by an exposure time of 1.5 min per 2° increment. For the four-circle diffractometer measurements the intensities of two reflections were monitored and no significant crystal deterioration was observed. Further data collection parameters are summarized in Table 8. The structures were solved by using the Patterson method (program XS).^{25} A series of full-matrix least-squares refinement cycles on F^2 (program SHELXL 93^{26}) followed by

Fourier syntheses gave the positions of all the remaining atoms. The hydrogen atoms in all four structures were placed at calculated positions and constrained to 'ride' on the atom to which they are attached. The isotropic thermal parameters for the methyl protons were refined with 1.5 times, and for all other hydrogen atoms 1.2 times, the U_{eq} value of the corresponding atom. All non-hydrogen atoms in the structures were refined anisotropically.

Atomic coordinates, thermal parameters and bond lengths and angles have been deposited at the Cambridge Crystallographic Data Centre (CCDC). See Instructions for Authors, *J. Chem. Soc., Dalton Trans.*, 1996, Issue 1. Any request to the CCDC for this material should quote the full literature citation and the reference number 186/55.

References

1 B. Lippert, *Prog. Inorg. Chem.*, 1989, **37**, 1.
2 J. P. Davidson, P. J. Faber, R. G. Fischer, jun., S. Mansy, H. J. Peresie, B. Rosenberg and L. van Camp, *Cancer Chemother. Rep., Part 1*, 1975, **59**, 287; B. Lippert, *J. Clin. Hematol. Oncol.*, 1977, **7**, 26.
3 G. Reusmann, M. Grehl, W. Reckordt and B. Krebs, *Z. Anorg. Allg. Chem.*, 1994, **620**, 199.
4 W. Kleiböhmer, B. Wenclawiak and B. Krebs, *2nd International Conference on the Chemistry of the Platinum Group Metals*, Edinburgh, 1984, Abstract C-3; J. Woltering W. Reckordt, W. Kleiböhmer and B. Krebs, *3rd International Conference on the Chemistry of the Platinum Group Metals*, Sheffield, 1987, Abstract H-7; G. Reusmann, M. Grehl, W. Reckordt and B. Krebs, *4th International Conference on the Chemistry of the Platinum Group Metals*, Cambridge, 1990, Abstract B-5; H. Engelking, S. Karentzopoulos, G. Reusmann and B. Krebs, *5th International Conference on the Chemistry of the Platinum Group Metals*, St. Andrews, 1993, Abstract B-59.
5 M. Grehl and B. Krebs, *Inorg. Chem.*, 1994, **33**, 3877.
6 H. Engelking, S. Karentzopoulos, G. Reusmann and B. Krebs, *Chem. Ber.*, 1994, **127**, 2355.
7 M. J. Bloemink, H. Engelking, N. Gütschow, S. Karentzopoulos, B. Krebs and J. Reedijk, *J. Inorg. Biochem.*, 1995, **59**, 222; M. J. Bloemink, H. Engelking, S. Karentzopoulos, B. Krebs and J. Reedijk, *Inorg. Chem.*, 1996, **35**, 619.
8 S. Karentzopoulos, H. Engelking, B. Bremer, N. Paschke and B. Krebs, *Acta Crystallogr., Sect. C*, in the press.
9 H. Engelking and B. Krebs, EUROBIC II, Metal Ions in Biological Systems, Florence, 1994, Abstract 349; H. Engelking, Doctoral thesis, Westfälische Wilhelms-Universität Münster, 1995.
10 A. J. Canty, E. E. George and C. V. Lee, *Aust. J. Chem.*, 1983, **36**, 415.
11 R. Faggiani, C. J. L. Lock, R. J. Pollock, B. Rosenberg and G. Turner, *Inorg. Chem.*, 1981, **20**, 804.
12 W. Micklitz, W. S. Sheldrick and B. Lippert, *Inorg. Chem.*, 1990, **29**, 211.
13 W. Micklitz, O. Renn, H. Schöllhorn, U. Thewalt and B. Lippert, *Inorg. Chem.*, 1990, **29**, 1836.
14 R. Faggiani, C. J. L. Lock, R. J. Pollock, B. Rosenberg and G. Turner, *Inorg. Chem.*, 1981, **20**, 804.
15 B. Lippert, D. Neugebauer and G. Raudaschl, *Inorg. Chim. Acta*, 1983, **78**, 161.
16 G. Trötscher, W. Micklitz, H. Schöllhorn, U. Thewalt and B. Lippert, *Inorg. Chem.*, 1990, **29**, 2541.
17 M. Grehl, Doctoral thesis, Westfälische Wilhelms-Universität Münster, 1992.
18 C. J. L. Lock, H. J. Peresie, B. Rosenberg and G. Turner, *J. Am. Chem. Soc.*, 1978, **100**, 3371.
19 D. Neugebauer and B. Lippert, *Inorg. Chim. Acta*, 1982, **67**, 151.
20 H. Schöllhorn, U. Thewalt and B. Lippert, *Inorg. Chim. Acta*, 1984, **93**, 19.
21 B. Lippert, D. Neugebauer and U. Schubert, *Inorg. Chim. Acta*, 1980, **46**, L11.
22 H. Schöllhorn, U. Thewalt and B. Lippert, *Inorg. Chim. Acta*, 1984, **93**, 19.
23 T. V. O'Halloran and S. J. Lippard, *Inorg. Chem.*, 1989, **28**, 1289; *J. Am. Chem. Soc.*, 1983, **105**, 3341; K. Matsumoto, H. Moriyama and K. Suzuki, *Inorg. Chem.*, 1990, **29**, 2096.
24 STOE IPDS software package, STOE & CIE, Darmstadt, 1993.
25 G. M. Sheldrick, SHELXTL PLUS, Siemens Analytical X-Ray Instruments, Madison, WI, 1990.
26 G. M. Sheldrick, SHELXL 93, Program for Crystal Structure Determination, University of Göttingen, 1993.